Hadronic Structure at the Luminosity Frontier

Introduction

The proposed energy upgrade to the CEBAF accelerator at the Thomas Jefferson National Accelerator Facility would enable the only facility worldwide, planned or foreseen, that can address the complexity at the scientific frontier of emergent hadron structure with its high luminosity and probing precision at the hadronic scale. While high energy facilities will illuminate the perturbative dynamics and discover the fundamental role of gluons in nucleons and nuclei, a medium energy electron accelerator at the luminosity frontier will be critical to understanding the rich and extraordinary variety of nonperturbative effects manifested in hadronic structure.

The Lagrangian of QCD, which we believe governs the dynamics of quarks and gluons, is not easily or directly connected to the complicated observables that we measure in electron-proton and electron-nuclear scattering experiments. At one end of the spectrum, the elementary quark/gluon degrees of freedom are manifest only at distances $\lesssim 0.1$ fm, where the quark-gluon interactions can be understood using methods of perturbation theory; however, at hadronic distances ~ 1 fm the dynamics undergo qualitative changes, causing the appearance of effective degrees of freedom expressed in new structure and dynamics. While these new structures develop in the context of the underlying QCD degrees of freedom, their experimental interpretation remains challenging. This places strong interaction physics in the context of, "emergent phenomena", a powerful paradigm for the study of complex systems used in other areas of physics such as condensed matter, as well as biological and social sciences. Here, the behavior of larger and complex aggregates of elementary particles may not be understood in terms of an extrapolation of the properties of a few particles. Instead, at each level of complexity, entirely new properties appear − and the understanding of each new behavior warrants study. This is demonstrated in Fig. 1 where the distance scale incorporates emergence.

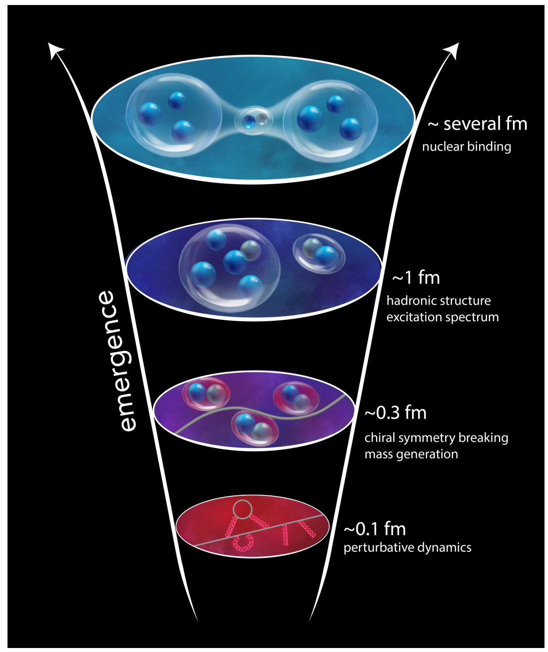

Figure 1: The emergence of structure in QCD from the perturbative regime of quarks and gluons to bound hadrons to hadrons bound in nuclei.

Experimental scattering observables are shaped by certain effects rooted in the quantum and nonlinear nature of QCD. These effects create dynamical scales not present in the original theory (see Fig. 1). One effect is the breaking of scale invariance by quantum fluctuations at high energies beyond the range of observation, which creates a mass/length scale that acts as the source of all other dynamical scales emerging from the theory (so-called trace anomaly). Another effect is the spontaneous breaking of chiral symmetry, which generates a dynamical mass of the quarks that provides most of the mass of the light hadrons, including the nucleon, and is therefore the source of 99% of the mass of the visible universe. Yet another effect is confinement, which limits the propagation of QCD color charges over hadronic distances and influences the long-range structure of hadrons and their excitation spectrum. Understanding these nonperturbative effects is the key to understanding the emergence of hadrons and nuclei from QCD.

Many expressions of these nonperturbative effects can be seen already in established hadron spectra and interactions. Chiral symmetry breaking is expressed in the unnaturally small mass of the pion, which emerges as the Goldstone boson mediating the long range QCD interactions, and its momentum-dependent coupling to other hadrons; confinement is visible in the spectra of heavy quarkonia. However, in order to truly understand "how" the effective dynamics emerges from QCD, it is necessary to observe the chromodynamic fields "at work" in these nonperturbative phenomena. This can be done through scattering processes probing hadron structure and spectra in energy-momentum regions where they are associated with nonperturbative dynamics. Formulating such processes has been a priority of theoretical and experimental research in recent years.

Since the 2015 Long-Range plan, several novel processes probing hadron structure and spectra have come into focus, revealing specific aspects of nonperturbative dynamics and providing insight into the emergence of structure from QCD. In concert, recent advances in accelerator science and technology have made possible a promising, cost-effective extension of the energy reach of the CEBAF accelerator to 22 GeV within the existing tunnel footprint. To map the emergence of hadronic structure from perturbative dynamics, several experimental requirements must be met. One is the need for a large four-momentum transfer, $Q > 2$ GeV, to have a well-controlled and localized probe (< 0.1 fm). Importantly, a second momentum scale is simultaneously needed to be sensitive to the emergent regime across the scales shown in Fig. 1. Such two-scale experimental observables are naturally accessible at a lepton-hadron facility like CEBAF, including exclusive electron-hadron deep virtual Compton scattering (DVCS): $e(\ell) + h(p) \to e(\ell') + h(p') + \gamma$ with the hard scale $Q^2 = -(\ell - \ell')^2$ and the second scale $t = (p - p')^2$, and semi-inclusive deep inelastic scattering (SIDIS): $e(\ell) + h(p) \to e(\ell') + h'(p') + X$ with the momentum imbalance between ℓ' and p' as the second scale. However, once the hadron is broken, larger momentum transfer Q leads to more collision induced radiation, which could significantly shadow the structure information probed at the second (and the soft) scale and reduce our precision to probe the emergent hadron structure. The requisite electron beam energy to probe hadron structure is determined by the need to, for instance, reach charm threshold in deep-virtual processes, and to separate produced hadronic systems from target remnants. Studies presented in this document show that the optimal beam energy for performing such two-scale measurements is ~ 20 GeV. Another determining constraint to the measurements is the need to precisely measure small cross sections in multidimensional phase space, needed also for separation of different dynamical mechanisms, which requires high luminosity and multiple devices with differing but complementary experimental capabilities. The fixed-target experiments with the CEBAF accelerator at JLab will achieve luminosities $\sim 10^{38}\text{cm}^{-2}\text{s}^{-1}$ with the high-resolution spectrometers and SoLID, and $\sim 10^{35}\text{cm}^{-2}\text{s}^{-1}$ with the CLAS12 large-acceptance detector. The foreseen Jefferson Lab experimental equipment, including SoLID in Hall A, high luminosity CLAS12 in Hall B, precision magnetic spectrometers in Hall C, and polarized, tagged photon beams in Hall D, matches the science need. It is a major advantage that the measurements can be performed using the existing and well-understood JLab12 detectors, reducing cost and minimizing technical risk to the program.

The experimental program proposed here is complementary and synergistic with both the current JLab 12 GeV program (including SOLID) and the future Electron-Ion Collider (EIC). It provides a critical bridge between the two, exploring fascinating and essential aspects of the emergence of hadrons that are needed for full understanding but are not covered by either JLab 12 GeV or the EIC. The center-of-mass energies reached in these fixed-target experiments ($\sqrt{s} \sim 6$ GeV) are still substantially below those reached in colliding-beam experiments at EIC ($\sqrt{s} > 20$ GeV), while the luminosity of the fixed target facilities is $\sim 3 - 4$ orders of magnitude larger. At the same time, there is considerable synergy between the scientific programs pursued with the upgraded CEBAF and the EIC. The experimental requirements for many of the measurements needed to answer the myriad questions posed by the emergence of structure have been assessed in simulations, and some highlights are described in the sections below.

Spectroscopy of Exotic States with $c\bar{c}$

The experimental discovery of a number of new exotic mesons and baryons lying in the charmonium energy region, labelled the $XYZP$, has caused a revolution in hadron spectroscopy, as these states challenge our previously successful ideas of how hadrons can be constructed from the quarks and gluons of QCD [1–4]. While a large literature has built up attempting to describe these new states, no single framework is capable of describing them all [5]. The lack of overlap between the set of states reported in e^+e^- annihilation [6–9], and those reported in B-decays [10–12], even for common final states, is not what one would expect for resonances, and has motivated non-resonant explanations for some signals [13].

All of the charged tetraquark candidates, labelled Z, are observed in processes with three hadrons in the final state, where the enhancement is seen in a two-hadron subchannel, but it is known that in this case peaks can occur for purely kinematical reasons [14–16], mimicking a resonance if the lineshape is not well resolved. In addition, in some of these three-hadron processes, the extraction of new exotic states can be very sensitive to required modeling of production of conventional resonances in the other two-hadron channels.

The experiments in which these states have been discovered, like LHCb, BESIII and Belle, will, in the near term, collect higher statistics in the discovery modes, and closely related processes. This will allow for improved resolution that may expose lineshape departures from the expectation of simple resonances [17], but these processes come with limitations. In B-decays the production is at a fixed three-body energy (the mass of the B meson), so the dependence of the production on that energy cannot be explored, and while the beam energy in e^+e^- annihilation can be scanned, production of particular Z_c states appears to happen only in certain center-of-mass energy regions. In comparison, *charge-exchange photoproduction* offers a clean environment for production of Z_c states via a $J/\psi\,\pi$ collision, where the photon provides the virtual J/ψ to scatter off the pion cloud around the proton, a process that is predicted to have a relatively large cross section at energies just above the threshold [18]. The Z_c can then decay to, for example, $J/\psi\,\pi$ without the complication of an overlapping third hadron. In this case, no complex three-hadron amplitude modeling is required, and any observation of a sharp enhancement away from the opening of a kinematic threshold would have an almost unambiguous interpretation as a resonance.

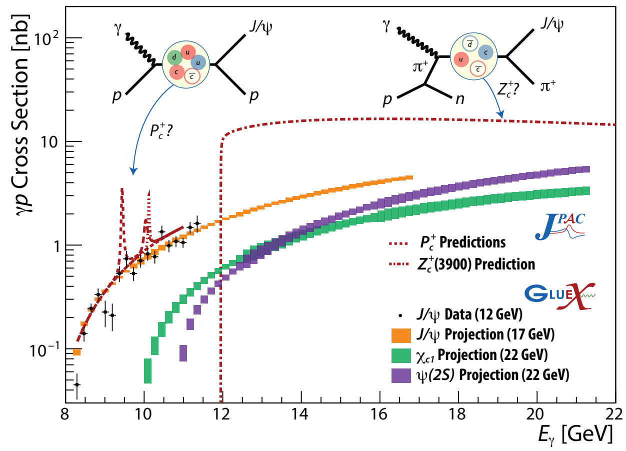

Figure 2: Photoproduction cross section vs. photon beam energy for various processes containing a $c\bar{c}$ pair. Data from GlueX are shown by black points. Projected GlueX precision for various electron energies are shown by boxes. Predictions for P_c and Z_c resonant signals are shown with dashed curves.

This philosophy of using photoproduction to validate observations made in three-hadron final states at high energy machines, has already been explored, albeit limited in energy reach, at the 12 GeV CEBAF, in the form of photoproduction of $J/\psi\,p$ in which the hidden-charm pentaquark candidates P_c observed in Λ_b decays at LHCb are expected [19]. The absence of signals for such states in recent GlueX [20] and Hall-C data puts rather severe constraints on their interpretation. With an energy upgraded CEBAF, this line of investigation can be extended to other exotic candidates that challenge our established pictures of hadron construction.

Bound Three Quark Structure of N^*s and Emergence of Mass

Understanding the strong interaction dynamics that govern the emergence of the nucleon ground and excited states N^*s, hence most of the visible mass in the Universe, is a challenging open problem in the QCD sector of the Standard Model that extends to all hadrons. Over the last decade, since the review of Ref. [21], essential progress has been achieved in the exploration of N^* electroexcitation amplitudes, the so-called

$\gamma_v pN^*$electrocouplings, stimulating research efforts [22–30] with an emphasis on how the structure of N^* states and their masses emerge from QCD. High-quality meson electroproduction data of the 6-GeV era at JLab from the CLAS detector have allowed for a reliable extraction of the electrocouplings of the most prominent N^*s in the mass range up to 1.8 GeV, as exemplified in Fig. 3. The data for different N^* states exhibits many facets of the strong interaction generating N^* structure and mass in Q^2 range up to 5 GeV^2 [22, 24–28, 31]. CLAS12 is the only foreseen facility capable of extending the results on the $\gamma_v pN^*$ electrocouplings into the unexplored Q^2 range from 5 to 10 GeV^2 based on measurements of πN, $\pi^+\pi^-p$, $K\Lambda$, and $K\Sigma$ electroproduction [22, 24], spanning the domain where up to ≈50% of the N^* mass is generated. Ultimately, pushing the momentum transfer to N^*s up to 30 GeV^2 will extend this coverage to where ≈90% of hadron mass emerges. In this regime where the QCD running coupling becomes small, direct comparisons of nonperturbative and pQCD concepts on how hadron structure emerges from QCD can be attempted. This unique endeavor of probing QCD through studies of N^* states is fully complementary to hard scattering off single quarks studied in deep inelastic scattering and paves the way for further extensions of the exploration of N^* structure in three dimensions [32]. Simulations of various electroproduction channels with an increased CEBAF beam energy of 22 GeV show that the electrocouplings can indeed be extracted up to $Q^2 \approx 30$ GeV^2 utilizing the large acceptance CLAS12 spectrometer at luminosities $\mathcal{L} \approx 2 - 5 \times 10^{35}$ cm^{-2}s^{-1} as exemplified in Fig. 3.

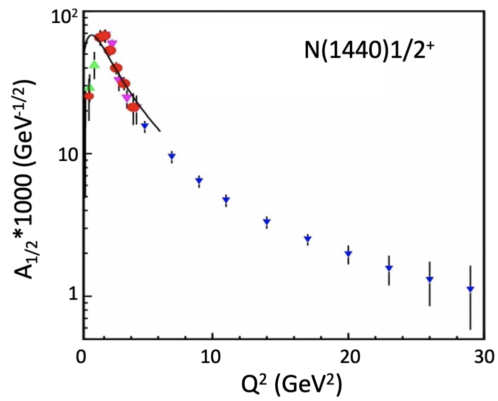

Figure 3: Available results at Q^2 up to 5 GeV^2 and those projected for the Q^2 evolution of the $N(1440)1/2^+$ $A_{1/2}$ electrocoupling for Q^2 up to 30 GeV^2 for a luminosity of 5×10^{35} cm^{-2}s^{-1} and six months of data collection time.

Spatial structure and mechanical properties of the proton

The extended spatial structure of hadrons is one of the basic expressions of their emergence from QCD. It attests to their composite nature and reveals the dynamical scales created by the non-perturbative phenomena (see Fig. 1). One source of information on the spatial structure are the form factors of operators measuring local physical quantities. While originally developed for the electromagnetic currents and the distribution of charge and magnetization, this concept has been extended to a much larger class of QCD operators composed from quark and gluon fields. The form factors of the QCD energy-momentum tensor (spin-2 quark and gluon operators) describe the spatial distributions of momentum, angular momentum, and forces in the nucleon and quantify the mechanical properties of the dynamical system [33, 34]. The form factor of the trace anomaly (spin-0 gluon operator) describes the spatial distribution of the gluonic fields involved in scale symmetry breaking and plays an important role in the proton mass decomposition [35–37]. Another source of information are the generalized parton distributions (GPDs) [38–40], which describe the spatial distributions of quarks and gluons in the transverse plane seen by a high-energy probe sampling field components with given longitudinal momentum. They create "tomographic images" of the hadron in terms of quark/gluon degrees of freedom and bring them to life as 3D objects in space.

Form factors and GPDs are measured in exclusive processes, where the initial hadron emerges intact in the final state, and the momentum transfer is conjugate to the spatial structure investigated. Such measurements require high luminosity because of low rates and the need for differential measurements. The proposed high-intensity 22 GeV facility would provide qualitatively new capabilities for exploring the spatial structure of hadrons in both gluon and quark degrees of freedom.

Gluonic form factors and trace anomaly from charmonium production. Exclusive photo- and electroproduction of heavy quarkonia provides a clean probe of the gluon field in the nucleon. Charmonium production at EIC energies ($W >\sim 10$ GeV) probes the gluon GPDs at $x <\sim 0.1$ [41]. Charmonium

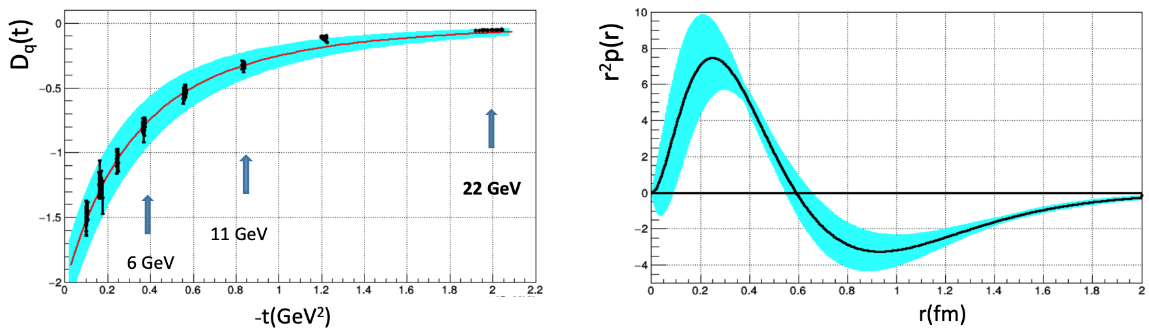

Figure 4: Left: The D-term form factor of the QCD energy-momentum tensor, $D_q(t)$, as a function of the momentum transfer $-t$, as extracted from DVCS experiments. The arrows indicate the $-t$ ranges covered at different beam energies with the constraint $-t/Q^2 < 0.2$. Right: Quark pressure distribution in the proton, $p(r)$, as a function of the distance from the proton center, r, obtained as the Fourier transform of $D_q(t)$.

production at near-threshold energies ($W - W_{\text{thr}} \sim$ 2–4 GeV) measures the form factors of local or almost local gluon operators probing the non-perturbative gluon fields in the nucleon, in various momentum and polarization projections, including operators of a type similar to the QCD trace anomaly [42–44]. This provides a unique window into the nonperturbative gluon fields in the nucleon and their connection with the valence quarks, and thus into the dynamical mass generation in QCD [35–37]. This field of research has expanded dramatically in the last 5 years, and further progress in theory is expected in the next 10 years. The 22 GeV energy is essential for opening up the phase space above the charm threshold and achieving sufficient energy/momentum transfers; the luminosity of $\sim 10^{37}$ cm^{-2} s^{-1} is critical for this low-rate process. Complementary measurements of near-threshold Υ production would be possible with the EIC at 100 fb^{-1} integrated luminosity with suitable detectors [41].

Mechanical structure from Deeply-Virtual Compton Scattering (DVCS). The form factors of the energy-momentum tensor are at the center of modern nucleon structure physics. Of particular interest is the D-term [45], which describes the distribution of QCD forces in the nucleon ("pressure") [46] and has become the subject of numerous theoretical studies of the "mechanical properties" of the nucleon [33, 34]. The D-term form factor appears as the subtraction constant in a dispersion relation of the amplitude of the DVCS process and be extracted from the experimental data on $ep \to e'\gamma p$ with minimal model dependence. First empirical extractions of the D-term and the "pressure" distribution have been performed with the JLab 6 GeV data (see Fig. 4) [47, 48]; further data will come from JLab 12 GeV. A definitive extraction of the D-term would be possible with the 22 GeV facility. The DVCS data in this energy range, together with the EIC data at higher energies [41], would provide complete energy coverage for the dispersion integral and permit tests of the stability of the subtraction. The high luminosity would allow one to extend the measurements to significantly higher values of t, which would for the first time test the high-t behavior of an energy-momentum tensor form factor, and permit reliable reconstruction of spatial distribution (see Fig. 4).

Fully differential 3D imaging of nucleon using dilepton production. The program of "tomographic imaging" of the nucleon with GPDs requires the full information on their dependence on the longitudinal momentum variables — the parton momentum fraction x, and the longitudinal momentum transfer ξ. Conventional exclusive processes such as DVCS cannot fully disentangle the x and ξ dependence, because the observables sample the GPDs only in the special kinematics of $x = \xi$ or as integrals over x. Novel processes such as dilepton production $ep \to e'(l^+l^-)p$, $l = e$ or μ (Double Deeply Virtual Compton Scattering, or DDVCS) can disentangle the longitudinal momentum variables in the GPDs by varying the dilepton mass in the process [49, 50]. By measuring the t-dependence in this configuration, they could provide fully differential tomographic images of nucleon structure. These next-generation measurements are challenging, and exploratory studies with JLab 12 GeV are under way [51]. The proposed 22 GeV facility would be ideally suited for this program. The energy is needed for reaching dilepton masses $M(l^+l^-) \sim$ few GeV in electroproduction with $Q^2 \sim$ few GeV^2; the luminosity is essential because the cross section is suppressed by a factor $\alpha_{\text{em}} \sim 10^{-2}$ compared to DVCS.

Fragmentation, Transverse Momentum and Parton Correlations

In Semi-Inclusive DIS (SIDIS), there are several independent structure functions (SFs) that characterize the production of hadrons as a function of beam and target polarizations. A subset of these SFs admits a connection to a rich variety of quantum correlation functions of quarks and gluons in momentum space via Transverse Momentum Dependent (TMD) factorization. The possibility to map out such correlation functions from data depends critically on our ability to measure independently each of these structure functions. However, the separation of SFs is highly non-trivial specially in the valence region at high energies, where the relative contributions from longitudinal and transverse photons, $\epsilon \to 1$. Also, in this domain, kinematic factors tend to suppress the signal of certain SFs e.g. helicity dependent SFs sensitive to longitudinal spin-dependent TMDs. A combined 11 and 22 GeV SIDIS program will increase our ability to measure a variety of SIDIS SFs across an enhanced multidimensional phase space and it will allow us to stress test and validate our understanding and interpretation of SIDIS reactions in QCD.

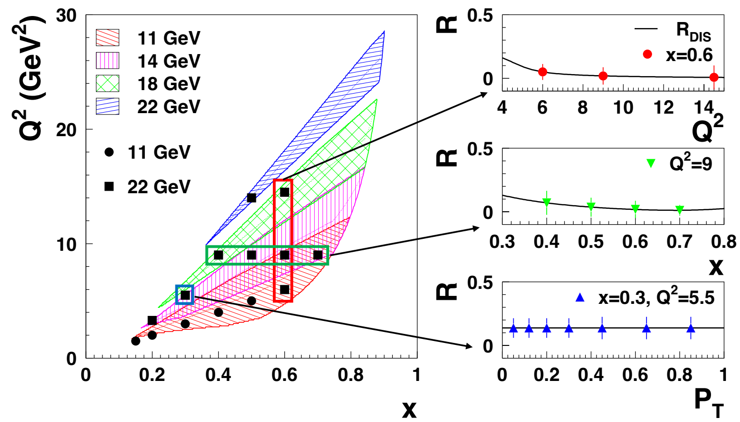

Figure 5: Phase space (left) and $R_{\rm SIDIS}$ projections (right) with the combined JLab 11 & 22 GeV at Hall C using $\Delta_{\rm min}\epsilon = 0.2$. The projected precision for $R_{\rm SIDIS}$ at the selected kinematics assumes point-to-point systematic errors of 1.4%. That accessibility for the full P_T range will require a combined analysis of Hall C and B.

Longitudinal photon contributions in SIDIS: While most of the SIDIS programs has been focused on understating SFs associated with transverse photons, the longitudinal SFs are relatively unknown and often ignored in TMD phenomenology. The combined JLab 11 and 22 GeV program will provide a unique determination of the ratio of longitudinal to transverse photon SIDIS cross sections ($R_{\rm SIDIS}$) as illustrated in Fig. 5. Such measurements will be essential to properly understand SIDIS multiplicities, Sivers and Collins effects to mention few. The latter has a broader impact in connection with nucleon tensor charges which plays an important role in search beyond the SM.

Accesibility to TMD physics: Interpretation of SIDIS data in terms of TMDs has been one the most pressing and challenging question in recent years [52–55]. One of the key leading factors is the inherent complexity of the reactions with multiple physical mechanisms that contribute to the production of hadrons in the final state. The connection of SIDIS data with TMDs is only within one of the mechanisms known as TMD *current region* and depending on the overall collision energy it overlaps with other mechanism such as target, central and hard collinear fragmentation regions [54, 56]. With an extended Q^2 coverage, the 22 GeV upgrade offers a new complementary window that sits in-between the 12 GeV program and the EIC (see Fig. 6), allowing precision multidimensional measurements in the full accessible phase space, enabling us to disentangle genuine intrinsic transverse structure of hadrons encoded in TMDs. Having two energies or in-between energy ranges will also identify scaling properties of the SIDIS reaction, to validate the measurements of leading contributions and explore sub-leading contributions associated with multi-parton interactions in QCD.

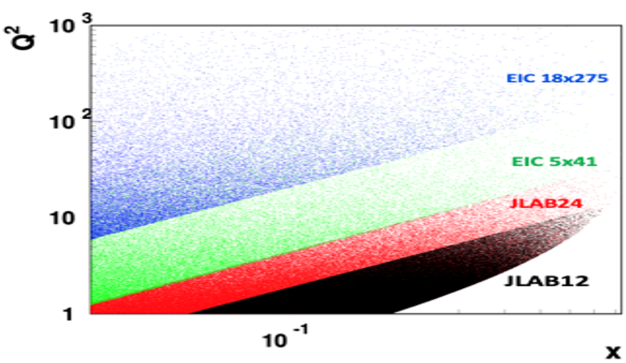

Figure 6: Combined kinematic coverage from JLab 12 GeV to EIC.

Hadron–Quark Transition and Nuclear Dynamics at Extreme Conditions

The proposed high energy and intensity beam upgrade will create an unprecedented opportunity for Nuclear Science to erase the knowledge gap between the dynamics of quark-gluon interactions and nuclear forces at short distances [57–59]. ***Two*** key directions that will significantly benefit from this upgrade are detailed below.

I. Nuclear Dynamics at Extreme Conditions

• **Probing the Nuclear Core:** While it has been understood since the 1950s that the stability of atomic nuclei is based on the existence of a repulsive core in the nucleon-nucleon interaction [60], the dynamics of such a core are still poorly understood. QCD offers a completely new perspective on the origin of the core, predicting the existence of nonnucleonic and hidden color components [61–64]. The energy upgrade will provide reach to the nuclear forces dominated by nuclear repulsion, see Fig. 7 **(a)**. The two main categories of experiments that will probe such distances are:

◇ **Superfast Quarks:** The unprecedentedly high Q^2 reach will allow 1) the suppression of quasi-elastic contributions, and correspondingly 2) the first-ever direct study of nuclear DIS structure function at $x > 1.2$ [65, 66], (Fig. 7 **(b)**). In this case, nuclear forces will be probed at ~ 0.5 fm, reaching the domain of the nuclear core [67–69].

◇ **Exploring Deuteron at Very Large Internal Momenta:** The deuteron structure will be studied at unprecedentedly large internal momenta ($>$ 800 MeV/c) and thus passing the threshold of inelastic excitations in the pn system [70, 71].

• **Probing Three-nucleon (3N) Forces:** 3N forces provide significant modification of the equation of state of high-density nuclear matter predicting the existence of neutron star masses exceeding two solar masses. Studying $A(e,\ e')X$ reactions at large Q^2 and $x > 2$ [72–74] as well as the electro-disintegration of $A = 3$ nuclei [75–77] will open up a new venue in the exploration of the dynamics of 3N forces.

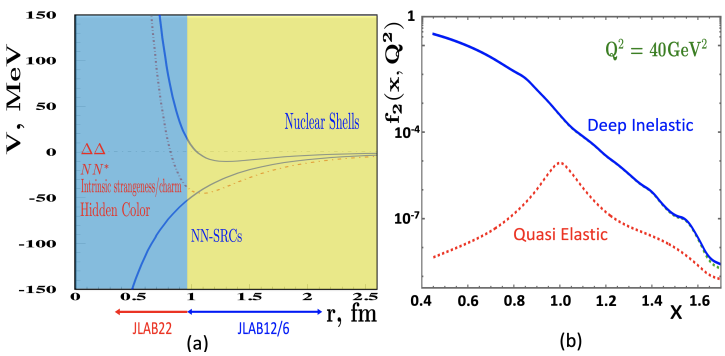

Figure 7: **(a)** Internucleon force reach at 22 GeV; **(b)** Suppression of quasi-elastic contributions.

II. Hadron-Quark Transition in Nuclear Medium

• **Investigation of Nuclear Medium Effects:** The emergence of nucleon interactions from QCD is also expressed in the "nuclear modifications" of the quark/gluon densities (characteristic differences from the densities in a sum of non-interacting nucleons), which attest to the QCD substructure of the NN interactions. Previous studies have focused on the valence quark densities in nuclei at $x > 0.3$ (the so-called EMC effect). Potentially as interesting are the nuclear modifications of quark/antiquark densities at $x \sim 0.1$ (the so-called antishadowing), which would attest to the QCD substructure of nuclear pions and other exchange interactions. The nuclear quark and antiquark densities can be measured using semi-inclusive or parity-violating inclusive DIS, opening a new window on nonnucleonic degrees of freedom in nuclei. A multifaceted study of nuclear medium phenomena at a wide range of Q^2 and x, see Fig. 8, using also polarized beams and targets with the ability to deploy numerous targets readily, will provide a breakthrough in understanding these effects. The goal of the exploration includes probing

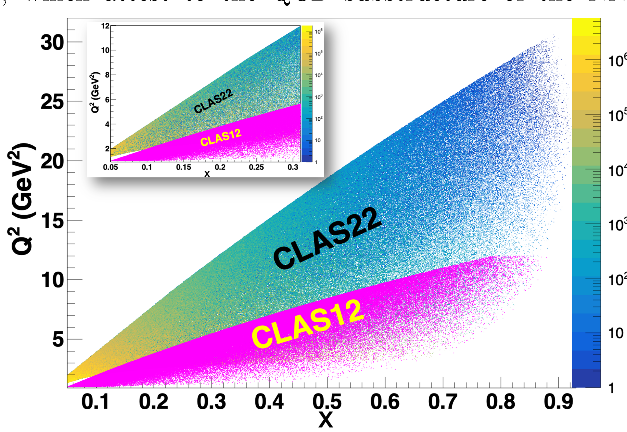

Figure 8: CLAS12 phase-space coverage at 22 GeV superimposed to 11 GeV, where the inset zooms in the antishadowing region (pink points not to scale).

1) nuclear antishadowing at $x \sim 0.1$ in which enhancement of nuclear PDFs is observed [78–82], 2) modification of polarization structure [82–88], and 3) medium modification of 3-D parton and bound nucleon structures [89–97].

• **Hadronization and Color Transparency (CT):** These studies aim at exploring two fundamental aspects related to QCD; 1) confinement dynamics and 2) the emergence of colorless strongly interacting hadrons. Extending the Q^2 range in CT studies will allow a deeper understanding of whether the colorless small-size three-quark system exhibits reduced interaction [98–102] as observed in $q\bar{q}$ systems [103–109]. In addition, dedicated studies of SIDIS production off nuclei with the unique luminosity of CEBAF will allow unprecedented investigations of QCD confinement dynamics, hadronization mechanisms, and quark-diquark correlations in nucleon structure [110–121] in a region complementary to EIC (See Fig. 6).

Partonic Structure and Spin

Nucleon Strangeness: The nucleon strange sector is largely unexplored with an up to 80% uncertainty in the $s^+ = s + \bar{s}$ PDF. Parity violating Deep Inelastic Scattering (PVDIS) of electrons offers a unique opportunity. Using the JAM framework [122], we found that a 22 GeV electron beam with the SoLID detector and a total of about 100 days of 40 μA beam split between 40 cm liquid deuterium and hydrogen targets would provide a substantial improvement, see Fig. 9. The reduction in the s^+ uncertainty can reach more than factor two at large-x. A similar experiment at 11 GeV would cover a comparable x-range, but the higher Q^2 with 22 GeV leads to relatively suppressed power corrections and a larger x region where data can be treated in a combined QED+QCD factorization framework [123]. More data at higher energy would be amenable to inclusion in various global PDF fits.

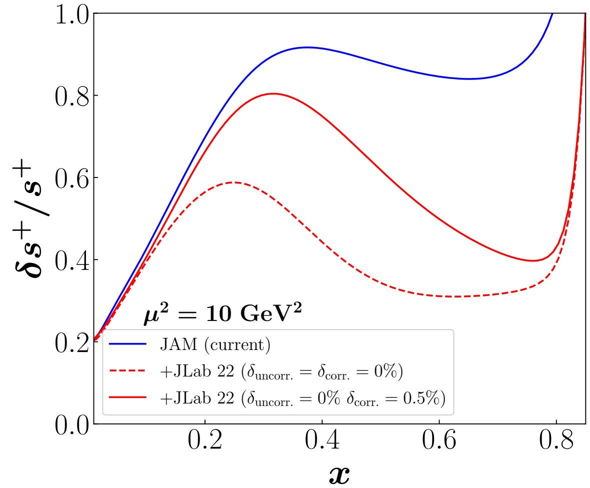

Figure 9: Impact of JLab 22 GeV A_{PV}^{DIS} data with the SoLID detector on nucleon's $s^+ = s + \bar{s}$ PDF.

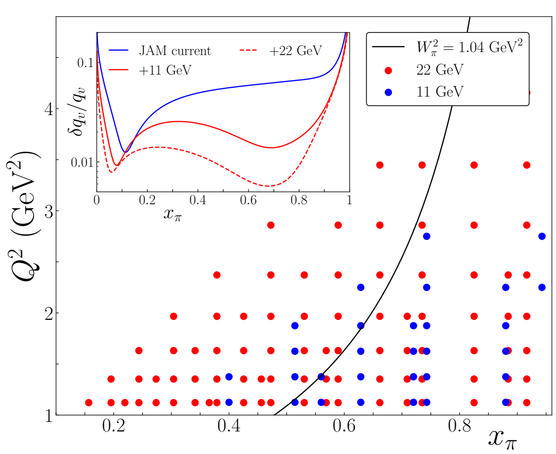

Figure 10: TDIS kinematics at JLab 11 and 22 GeV and the projected uncertainty on the pion's valence PDFs in logarithmic scale.

Meson Structure: Tagged deep inelastic scattering (TDIS) provides a mechanism to access meson structure via the Sullivan process [124–126]. These measurements will be amongst only a few to study the essentially unknown and yet fundamental emergence of meson structure. By probing low meson virtualites, the proposed programs at JLab and EIC will enable unique capabilities to deconvolute the partonic structure of mesons from TDIS measurements. For the case of pions, a cut of $W_\pi^2 > 1.04$ GeV^2 is needed to avoid contributions from resonances, which excludes most of the 11 GeV data. Such phase space limitation is avoided with the 22 GeV program, and projected impact studies on pion PDFs show a potential to improve the determination of the valence structure as illustrated in Fig. 10 insert. The data will span the transition to the bound regimes of resonances, complementary to 11 GeV enabling to explore quark-hadron duality in the meson sector. At a 22 GeV, the measurements would also kinematically overlap the existing pion induced Drell-Yan data for universality tests of PDFs in the mid-to large-x_π region. The proposed upgrade will extend the kinematic coverage to smaller x_π region to probe the sea content of mesons complementary to the EIC program. The determination of partonic structure of mesons will critically rely on measurements at Jefferson Lab in order to firmly constrain its valence regime and maximally control its extraction in the mid- to small-x_π regime at the EIC. In addition, the TDIS data can probe partonic structure of kaons which are currently unknown. Analogous to the case of pions, such measurements will require the 22 GeV upgrade in order access kinematic regions away from K^* resonances.

Precision α_S measurement: Polarized DIS on proton and neutron can provide a precision determination of the strong coupling α_s via the Bjorken Sum Rule. Combining projected JLab 22 GeV data with projected EIC data, one could determine α_s with a precision of 0.6%, which is more than a factor of 2 better than any single determination reported by the Particle Data Group[127, 128] and a factor of 3 better than the extraction with EIC data alone. The world combined determination would improve from the current precision of 0.85% to 0.5%.

QCD Confinement and Fundamental Symmetries

The JLab 22 GeV upgrade will enable precision measurements of the radiative widths and the transition form factors of π^0, η, and η' via the Primakoff effect to test QCD confinement and fundamental symmetries with experimental sensitivities not previously achievable. While π^0 and η are Goldstone bosons due to spontaneous chiral symmetry breaking, η' is not because of the $U(1)_A$ anomaly coupling to the gluon field. The axial anomaly coupling to the electromagnetic field drives the two-photon decays of π^0, η and η'. The decays of these mesons harbor fundamental information about the effects of SU(3) symmetry and the mixing phenomena of the mesons due to isospin and SU(3) symmetry breakings [129]. They offer a unique way to determine the fundamental parameters of QCD in a model-independent manner, such as the light quark-mass ratio and the mixing angle of η-η'. They also provide critical inputs to the theoretical calculations of the hadronic light-by-light contribution to the anomalous magnetic moment of the muon [130].

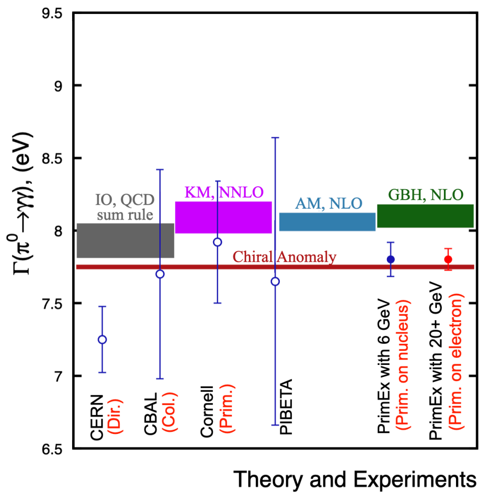

Figure 11: The projected $\Gamma(\pi^0 \to \gamma\gamma)$ with an atomic electron target (in red) and the previous published results (in blue).

Primakoff Production of π^0 off Atomic Electron: As the lightest hadron, π^0 plays a special role in our understand of QCD confinement. Its radiative decay width is one of very rare parameters in low-energy QCD that can be predicted at $\approx 1\%$ precision. The most accurate measurement of this fundamental parameter was from two Primakoff experiments (PrimEx I and II) [135] off nuclear targets (^{12}C, ^{28}Si and ^{208}Pb) at JLab 6 GeV. This result, shown as a solid blue point in Fig. 11, agrees to the leading-order chiral anomaly prediction [136] and is 2σ below the theoretical calculations [137–140] based on higher-order corrections to the anomaly.

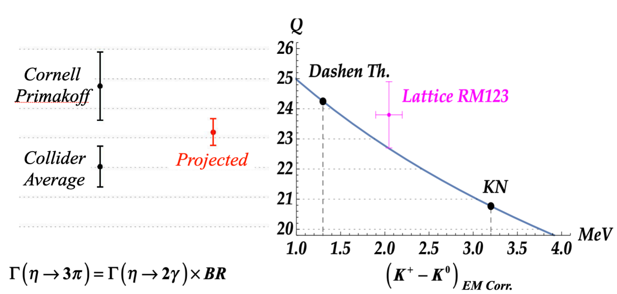

Figure 12: The quark mass ratio Q determined by two methods. The left-side are calculated from $\Gamma(\eta \to 3\pi)$ determined by using the values of previous experiments [131, 132] and the projected JLab 22 GeV for $\Gamma(\eta \to 2\gamma)$. The right-side are obtained from the kaon mass difference with theoretical EM corrections [129, 133, 134].

The threshold for photo- or electro-production of π^0 off an electron target is 18 GeV. The future JLab 22 GeV upgrade will thus enable measurements of radiative decay width and transition form factor of π^0 off an electron for the first time. An atomic electron target offers significant advantages over a nuclear target for the Primakoff experiments by eliminating all nuclear backgrounds, the largest systematic uncertainty in the previous PrimEx result [135]. The resulting expected precision on $\Gamma(\pi^0 \to \gamma\gamma)$, as shown in Fig. 11 (the red point), is necessary to better understand the discrepancy between the existing experimental result and the high-order QCD predictions.

Primakoff Productions off Nuclear Target:

A higher beam energy will increase the Primakoff cross section and improve the separation of the Primakoff signal from the nuclear backgrounds for the case of nuclear target. The 22 GeV upgrade thus will greatly enhance the Primakoff experiments for more massive mesons produced off nuclear targets. This will enable the first Primakoff measurement of $\Gamma(\eta' \to \gamma\gamma)$ with ∼3.5% precision to study the $U(1)_A$ anomaly coupling to the gluon field, and improve the measurement of $\Gamma(\eta \to \gamma\gamma)$ to a 2% accuracy to determine the light-quark mass ratio ($Q^2 = \frac{m_s^2 - \hat{m}^2}{m_d^2 - m_u^2}$) model-independently, as shown in Fig. 12 (in red).

A Technically Feasible, Cost Effective, Innovative Path to 22 GeV

Recent advances in accelerator technology have made it possible to extend the energy reach of the CEBAF accelerator up to 22 GeV within the existing tunnel footprint. Such an increase can be achieved by increasing the number of recirculations through the accelerating cavities. Encouraged by the recent success of the CBETA project (Cornell Brookhaven Electron Test Accelerator), a proposal was formulated to increase the CEBAF energy from the present 12 GeV to about 22 GeV by replacing the highest-energy arcs with Fixed Field Alternating Gradient (FFA) arcs.

The new pair of arcs configured with an FFA lattice would support simultaneous transport of 6 passes with energies spanning a factor of two. This wide energy bandwidth could be achieved using the non-scaling FFA principle implemented with Halbach-style permanent magnets. This novel magnet technology saves energy and lowers operating costs. Such a scheme would nearly double the energy while using the existing CEBAF SRF cavity system.

The design is based on an exciting new approach in accelerating electrons efficiently with multiple passes in a single FFA beam line. The Non-Scaling FFA approach allows beam acceleration within a small beam pipe size as in synchrotrons, but without varying the magnetic field. Different energy beams are transported in a small beam pipe with very small transverse orbit offsets due to the small dispersion function.

In addition to the spreaders, one must design the time-of-flight splitters for each of the energies which pass through the FFA arcs. These will be located along the new FFA arcs, downstream of the spreaders. This would necessitate four time-of-flight splitters, which are capable of adjusting the momentum compaction, M56, at both ends of each FFA arc. One of the challenges of the multi-pass (10+) linac optics is to provide uniform focusing in a vast range of energies, using fixed field lattice. Here, we configured a building block of linac optics as a sequence of two triplet cells with reversed quad polarities flanking two cryomodules. Initial triplets, configured with 45 Tesla/m quads, are scaled with increasing momentum along the linac. This style linac optics provides a stable periodic solution covering energy ratio 1:33. The current CEBAF is configured with a 123 MeV injector feeding into a racetrack recirculating linear accelerator (RLA) with a 1090 MeV linac on each side. The 123 MeV minimum makes optical matching in the first linac virtually impossible due to extremely high energy span ratio (1:175). Thus, it is proposed to replace the current injector with a 650 MeV 3-pass recirculating injector based on the existing LERF facility augmented by three C-70 cryomodules.

Staying within the CEBAF footprint, while transporting high energy beams (10-22 GeV) calls for special mitigation of synchrotron radiation effects. One of them is to increase the bend radius at the arc dipoles (packing factor of the FFA arcs increased to about 87.6) to suppress adverse effects of the synchrotron radiation on beam quality: dilution of the transverse and longitudinal emittance due to quantum excitations. Proposed 22 GeV, 10-pass, design would promise to deliver a normalized emittance of 76 mm mrad with a relative energy spread of 10-3. Further recirculation beyond 22 GeV is limited by large, 974 MeV per electron, energy loss due to synchrotron radiation, which depends on energy to the fourth power.

Finally, given the greater total energies expected with this upgrade, we are also investigating the impact this will have on our extraction system and beam delivery to the experimental halls. For the extraction system, this will depend partly on the needs of the experimental program, and partly on how we choose to extract the beam. For the beam delivery to the halls, the hall beam-lines are currently under investigation. Improvements to the magnetic septa are expected to be required, and the dipoles to the hall lines will need to be strengthened and improved as well. The overall optics will require some adjustments, but should be manageable, assuming that the beam is extracted.

Realization of an FFA-based 22 GeV upgrade will open not only a new era of the CEBAF science program, but the requisite scaling of this technology to higher energies will spur the development and demonstration of engineering solutions for FFA beamlines and permanent magnets that can be applied in many other energy efficient accelerators for scientific, environmental or medical applications. *It is important to note that demonstrating the ability to scale FFA technology up in energy is critical to the above planning and science. At this point, Jefferson Lab proposes to work on this critical step in the near future, with a longer timeline (discussed below) for the full upgrade.*

Preliminary Cost and Schedule Estimates for the 22 GeV Upgrade

The scientific reach of a 22 GeV upgrade as described in previous sections can fit in a particular time frame and budget envelope as illustrated in Fig. 13. The starting point is to recognize that the EIC will require about \$150M/year in new funding (assuming the V3 profile of the EIC project) starting in FY2024 and lasting until FY2029, at which point new funds for EIC will begin to ramp down. In this V3 scenario, and in the spirit of the BNL/JLab EIC partnership, the new EIC construction funding is equally split between JLab and BNL EIC project scope. The key to executing this approach is to capture the roll-off of EIC funding coming to JLab to pursue the CEBAF 22 GeV upgrade. A secondary assumption is that natural NP programmatic growth and project roll-off funds at BNL will cover the operations costs of the EIC. Presuming that programmatic and community support for the JLab 22 GeV upgrade sustains over the next decade, some small R&D funding will be necessary to prepare for the energy upgrade. We estimate \$3M/year starting in FY2025 for this R&D package which is currently in development. The R&D package will cover source work for the positron aspect of the upgrade, and FFA magnet work at high electron-beam energies.

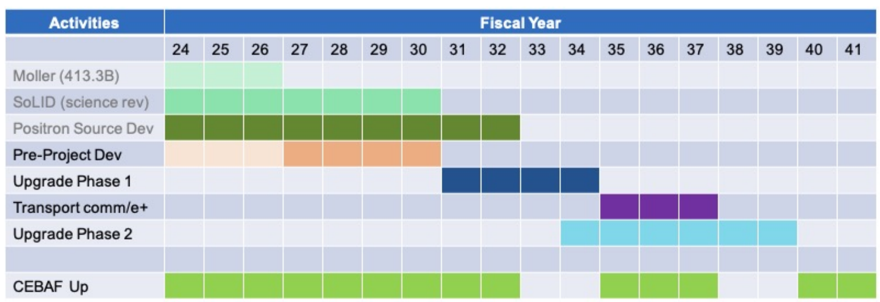

Figure 13: Timelines are shown for JLab activities through the energy upgrade. MOLLER and SoLID are shown, as well as R&D for the 12 GeV positron source, and energy upgrades. Also shown is a plan for CEBAF operations running through FY2042.

For completeness, Fig. 13 also includes current timelines anticipated for the ongoing MOLLER project and the anticipated SoLID project. MOLLER, a DOE O413.3B project is approaching CD-2/3, and should be complete by FY26. SoLID has been through an NP science review and awaits CD-0 from DOE. Positron source development is considered an off-project, and will entail continuing R&D to prepare a positron source for the 12 GeV effort during Phase 1 of the upgrade. Phase 1 of the upgrade involves the installation of a beamline from the LERF facility at JLab to CEBAF, and the installation of positron beam capabilities at 12 GeV. Positrons will run for 3 years at 12 GeV before the FFA magnet installation and injector upgrades (Phase 2) bring CEBAF to 22 GeV.

JLab engineers and accelerator scientists spent the last six months generating an initial cost estimate for the 22 GeV upgrade based on Fixed-Field Alternating Gradient (FFAG) technology, and including a positron phase. JLab estimates that the point cost estimate in FY23 dollars is \$345M with a range of \$265M to \$517M. Estimated costs of R&D to demonstrate the technology is on the order of \$9M over the next 3 years.

References

[1] Stephen Lars Olsen, Tomasz Skwarnicki, and Daria Zieminska. Nonstandard heavy mesons and baryons: Experimental evidence. *Rev. Mod. Phys.*, 90(1):015003, 2018. doi: 10.1103/RevModPhys.90.015003.

[2] Richard F. Lebed, Ryan E. Mitchell, and Eric S. Swanson. Heavy-Quark QCD Exotica. *Prog. Part. Nucl. Phys.*, 93:143–194, 2017. doi: 10.1016/j.ppnp.2016.11.003.

[3] Matthew R. Shepherd, Jozef J. Dudek, and Ryan E. Mitchell. Searching for the rules that govern hadron construction. *Nature*, 534(7608):487–493, 2016. doi: 10.1038/nature18011.

[4] R. A. Briceno et al. Issues and Opportunities in Exotic Hadrons. *Chin. Phys. C*, 40(4):042001, 2016. doi: 10.1088/1674-1137/40/4/042001.

[5] Nora Brambilla, Simon Eidelman, Christoph Hanhart, Alexey Nefediev, Cheng-Ping Shen, Christopher E. Thomas, Antonio Vairo, and Chang-Zheng Yuan. The XYZ states: experimental and theoretical status and perspectives. *Phys. Rept.*, 873:1–154, 2020. doi: 10.1016/j.physrep.2020.05.001.

[6] Medina Ablikim et al. Observation of a Near-Threshold Structure in the K^+ Recoil-Mass Spectra in $e^+e^- \to K^+(D_s^- D^{*0} + D_s^{*-} D^0)$. *Phys. Rev. Lett.*, 126(10):102001, 2021. doi: 10.1103/PhysRevLett.126.102001.

[7] M. Ablikim et al. Observation of a Charged Charmoniumlike Structure in $e^+e^- \to \pi^+\pi^- J/\psi$ at $\sqrt{s}$ =4.26 GeV. *Phys. Rev. Lett.*, 110:252001, 2013. doi: 10.1103/PhysRevLett.110.252001.

[8] M. Ablikim et al. Observation of a Charged Charmoniumlike Structure $Z_c(4020)$ and Search for the $Z_c(3900)$ in $e^+e^- \to \pi^+\pi^- h_c$. *Phys. Rev. Lett.*, 111(24):242001, 2013. doi: 10.1103/PhysRevLett.111.242001.

[9] Z. Q. Liu et al. Study of $e^+e^- \to \pi^+\pi^- J/\psi$ and Observation of a Charged Charmoniumlike State at Belle. *Phys. Rev. Lett.*, 110:252002, 2013. doi: 10.1103/PhysRevLett.110.252002. [Erratum: Phys.Rev.Lett. 111, 019901 (2013)].

[10] Roel Aaij et al. Observation of New Resonances Decaying to $J/\psi K^+ +$ and $J/\psi\phi$. *Phys. Rev. Lett.*, 127(8):082001, 2021. doi: 10.1103/PhysRevLett.127.082001.

[11] K. Chilikin et al. Experimental constraints on the spin and parity of the $Z(4430)^+$. *Phys. Rev. D*, 88 (7):074026, 2013. doi: 10.1103/PhysRevD.88.074026.

[12] Roel Aaij et al. Observation of the resonant character of the $Z(4430)^-$ state. *Phys. Rev. Lett.*, 112 (22):222002, 2014. doi: 10.1103/PhysRevLett.112.222002.

[13] Feng-Kun Guo, Xiao-Hai Liu, and Shuntaro Sakai. Threshold cusps and triangle singularities in hadronic reactions. *Prog. Part. Nucl. Phys.*, 112:103757, 2020. doi: 10.1016/j.ppnp.2020.103757.

[14] Feng-Kun Guo, Ulf G. Meißner, Juan Nieves, and Zhi Yang. Remarks on the P_c structures and triangle singularities. *Eur. Phys. J. A*, 52(10):318, 2016. doi: 10.1140/epja/i2016-16318-4.

[15] Melahat Bayar, Francesca Aceti, Feng-Kun Guo, and Eulogio Oset. A Discussion on Triangle Singularities in the $\Lambda_b \to J/\psi K^- p$ Reaction. *Phys. Rev. D*, 94(7):074039, 2016. doi: 10.1103/PhysRevD.94.074039.

[16] Satoshi X. Nakamura. $P_c(4312)^+$, $P_c(4380)^+$, and $P_c(4457)^+$ as double triangle cusps. *Phys. Rev. D*, 103:111503, 2021. doi: 10.1103/PhysRevD.103.L111503.

[17] A. Pilloni, C. Fernandez-Ramirez, A. Jackura, V. Mathieu, M. Mikhasenko, J. Nys, and A. P. Szczepaniak. Amplitude analysis and the nature of the $\mathrm{Z}_c(3900)$. *Phys. Lett. B*, 772:200–209, 2017. doi: 10.1016/j.physletb.2017.06.030.

[18] D. Winney, A. Pilloni, V. Mathieu, A. N. Hiller Blin, M. Albaladejo, W. A. Smith, and A. Szczepaniak. XYZ spectroscopy at electron-hadron facilities. II. Semi-inclusive processes with pion exchange. *Phys. Rev. D*, 106(9):094009, 2022. doi: 10.1103/PhysRevD.106.094009.

[19] A. N. Hiller Blin, C. Fernández-Ramírez, A. Jackura, V. Mathieu, V. I. Mokeev, A. Pilloni, and A. P. Szczepaniak. Studying the $\mathrm{P}_c(4450)$ resonance in J/ψ photoproduction off protons. *Phys. Rev. D*, 94 (3):034002, 2016. doi: 10.1103/PhysRevD.94.034002.

[20] A. Ali et al. First Measurement of Near-Threshold J/ψ Exclusive Photoproduction off the Proton. *Phys. Rev. Lett.*, 123(7):072001, 2019. doi: 10.1103/PhysRevLett.123.072001.

[21] I. G. Aznauryan et al. Studies of Nucleon Resonance Structure in Exclusive Meson Electroproduction. *International Journal of Modern Physics E*, 22(06):1330015, jun 2013. doi: 10.1142/s0218301313300154. URL https://doi.org/10.1142/S0218301313300154.

[22] Daniel S. Carman, Ralf W. Gothe, Victor I. Mokeev, and Craig D. Roberts. Nucleon Resonance Electroexcitation Amplitudes and Emergent Hadron Mass – arXiv:2301.07777 [hep-ph]. 2023.

[23] M. Yu. Barabanov et al. Diquark correlations in hadron physics: Origin, impact and evidence. *Progress in Particle and Nuclear Physics*, 116:103835, jan 2021. doi: 10.1016/j.ppnp.2020.103835. URL https://doi.org/10.1016/j.ppnp.2020.103835.

[24] S. J. Brodsky et al. Strong QCD from Hadron Structure Experiments: Newport News, VA, USA, November 4-8, 2019. *Int. J. Mod. Phys. E*, 29(08):2030006, 2020.

[25] Volker D. Burkert. Nucleon Resonances and Transition Form Factors – arXiv:2212.08980 [hep-ph]. 2022.

[26] Volker D. Burkert and Craig D. Roberts. Colloquium : Roper Resonance: Toward a Solution to the Fifty Year Puzzle. *Rev. Mod. Phys.*, 91(1):011003, 2019.

[27] Victor I. Mokeev and Daniel S. Carman. Photo- and Electrocouplings of Nucleon Resonances. *Few Body Syst.*, 63(3):59, 2022.

[28] D. S. Carman, K. Joo, and V. I. Mokeev. Strong QCD Insights from Excited Nucleon Structure Studies with CLAS and CLAS12. *Few Body Syst.*, 61(3):29, 2020.

[29] Craig D Roberts. Empirical Consequences of Emergent Mass. *Symmetry*, 12(9):1468, 2020.

[30] Craig D. Roberts. On Mass and Matter. *AAPPS Bull.*, 31:6, 2021.

[31] I. G. Aznauryan and V. D. Burkert. Electroexcitation of Nucleon Resonances. *Prog. Part. Nucl. Phys.*, 67:1–54, 2012.

[32] V. D. Burkert et al. Precision Studies of QCD in the Low Energy Domain of the EIC. 11 2022.

[33] Maxim V. Polyakov and Peter Schweitzer. Forces inside hadrons: pressure, surface tension, mechanical radius, and all that. *Int. J. Mod. Phys. A*, 33(26):1830025, 2018. doi: 10.1142/S0217751X18300259.

[34] Cédric Lorcé, Hervé Moutarde, and Arkadiusz P. Trawiński. Revisiting the mechanical properties of the nucleon. *Eur. Phys. J. C*, 79(1):89, 2019. doi: 10.1140/epjc/s10052-019-6572-3.

[35] Cédric Lorcé. On the hadron mass decomposition. *Eur. Phys. J. C*, 78(2):120, 2018. doi: 10.1140/epjc/s10052-018-5561-2.

[36] Yoshitaka Hatta, Abha Rajan, and Kazuhiro Tanaka. Quark and gluon contributions to the QCD trace anomaly. *JHEP*, 12:008, 2018. doi: 10.1007/JHEP12(2018)008.

[37] Andreas Metz, Barbara Pasquini, and Simone Rodini. Revisiting the proton mass decomposition. *Phys. Rev. D*, 102(11):114042, 2021. doi: 10.1103/PhysRevD.102.114042.

[38] K. Goeke, Maxim V. Polyakov, and M. Vanderhaeghen. Hard exclusive reactions and the structure of hadrons. *Prog. Part. Nucl. Phys.*, 47:401–515, 2001. doi: 10.1016/S0146-6410(01)00158-2.

[39] M. Diehl. Generalized parton distributions. *Phys. Rept.*, 388:41–277, 2003. doi: 10.1016/j.physrep.2003.08.002.

[40] A. V. Belitsky and A. V. Radyushkin. Unraveling hadron structure with generalized parton distributions. *Phys. Rept.*, 418:1–387, 2005. doi: 10.1016/j.physrep.2005.06.002.

[41] R. Abdul Khalek et al. Science Requirements and Detector Concepts for the Electron-Ion Collider: EIC Yellow Report. *Nucl. Phys. A*, 1026:122447, 2022. doi: 10.1016/j.nuclphysa.2022.122447.

[42] D. Kharzeev, H. Satz, A. Syamtomov, and G. Zinovjev. J/ψ photoproduction and the gluon structure of the nucleon. *Eur. Phys. J. C*, 9:459–462, 1999. doi: 10.1007/s100529900047.

[43] Oleksii Gryniuk and Marc Vanderhaeghen. Accessing the real part of the forward J/ψ-p scattering amplitude from J/ψ photoproduction on protons around threshold. *Phys. Rev. D*, 94(7):074001, 2016. doi: 10.1103/PhysRevD.94.074001.

[44] Kiminad A. Mamo and Ismail Zahed. Diffractive photoproduction of J/ψ and Υ using holographic QCD: gravitational form factors and GPD of gluons in the proton. *Phys. Rev. D*, 101(8):086003, 2020. doi: 10.1103/PhysRevD.101.086003.

[45] Maxim V. Polyakov and C. Weiss. Skewed and double distributions in pion and nucleon. *Phys. Rev. D*, 60:114017, 1999. doi: 10.1103/PhysRevD.60.114017.

[46] M. V. Polyakov. Generalized parton distributions and strong forces inside nucleons and nuclei. *Phys. Lett. B*, 555:57–62, 2003. doi: 10.1016/S0370-2693(03)00036-4.

[47] V. D. Burkert, L. Elouadrhiri, and F. X. Girod. The pressure distribution inside the proton. *Nature*, 557(7705):396–399, 2018. doi: 10.1038/s41586-018-0060-z.

[48] H. Moutarde, P. Sznajder, and J. Wagner. Unbiased determination of DVCS Compton Form Factors. *Eur. Phys. J. C*, 79(7):614, 2019. doi: 10.1140/epjc/s10052-019-7117-5.

[49] M. Guidal and M. Vanderhaeghen. Double deeply virtual Compton scattering off the nucleon. *Phys. Rev. Lett.*, 90:012001, 2003. doi: 10.1103/PhysRevLett.90.012001.

[50] Andrei V. Belitsky and Dieter Mueller. Exclusive electroproduction of lepton pairs as a probe of nucleon structure. *Phys. Rev. Lett.*, 90:022001, 2003. doi: 10.1103/PhysRevLett.90.022001.

[51] S. Zhao, A. Camsonne, D. Marchand, M. Mazouz, N. Sparveris, S. Stepanyan, E. Voutier, and Z. W. Zhao. Double deeply virtual Compton scattering with positron beams at SoLID. *Eur. Phys. J. A*, 57 (7):240, 2021. doi: 10.1140/epja/s10050-021-00551-3.

[52] J. O. Gonzalez-Hernandez, T. C. Rogers, N. Sato, and B. Wang. Challenges with Large Transverse Momentum in Semi-Inclusive Deeply Inelastic Scattering. *Phys. Rev. D*, 98(11):114005, 2018. doi: 10.1103/PhysRevD.98.114005.

[53] B. Wang, J. O. Gonzalez-Hernandez, T. C. Rogers, and N. Sato. Large Transverse Momentum in Semi-Inclusive Deeply Inelastic Scattering Beyond Lowest Order. *Phys. Rev. D*, 99(9):094029, 2019. doi: 10.1103/PhysRevD.99.094029.

[54] M. Boglione, J. Collins, L. Gamberg, J. O. Gonzalez-Hernandez, T. C. Rogers, and N. Sato. Kinematics of Current Region Fragmentation in Semi-Inclusive Deeply Inelastic Scattering. *Phys. Lett. B*, 766: 245–253, 2017. doi: 10.1016/j.physletb.2017.01.021.

[55] J. Collins, L. Gamberg, A. Prokudin, T. C. Rogers, N. Sato, and B. Wang. Relating Transverse Momentum Dependent and Collinear Factorization Theorems in a Generalized Formalism. *Phys. Rev. D*, 94(3):034014, 2016. doi: 10.1103/PhysRevD.94.034014.

[56] M. Boglione, A. Dotson, L. Gamberg, S. Gordon, J. O. Gonzalez-Hernandez, A. Prokudin, T. C. Rogers, and N. Sato. Mapping the Kinematical Regimes of Semi-Inclusive Deep Inelastic Scattering. *JHEP*, 10:122, 2019. doi: 10.1007/JHEP10(2019)122.

[57] S.J. Brodsky. Nuclear chromodynamics: applications of quantum chromodynamics to few nucleon systems. *Comments Nucl. Part. Phys.*, 12(5-6):213–241, 1984.

[58] L.L. Frankfurt and M.I. Strikman. Hard nuclear processes and microscopic nuclear structure. *Phys. Rept.*, 160(5):235–427, 1988. doi: 10.1016/0370-1573(88)90179-2.

[59] M.M. Sargsian et al. Hadrons in the nuclear medium. *J. Phys. G: Nucl. Part. Phys.*, 29(3):R1, 2003. doi: 10.1088/0954-3899/29/3/201.

[60] R. Jastrow. On the nucleon-nucleon interaction. *Phys. Rev.*, 81:165–170, 1951. doi: 10.1103/PhysRev.81.165.

[61] M. Harvey. Effective nuclear forces in the quark model with delta and hidden-color channel coupling. *Nucl. Phys. A*, 352(3):326–342, 1981. doi: https://doi.org/10.1016/0375-9474(81)90413-9.

[62] Ch.R. Ji and S.J. Brodsky. Quantum-chromodynamic evolution of six-quark states. *Phys. Rev. D*, 34:1460–1473, 1986. doi: 10.1103/PhysRevD.34.1460.

[63] L.L. Frankfurt and M.I. Strikman. High-energy phenomena, short-range nuclear structure and QCD. *Phys. Rept.*, 76(4):215–347, 1981. doi: https://doi.org/10.1016/0370-1573(81)90129-0.

[64] G.A. Miller. Pionic and hidden-color, six-quark contributions to the deuteron b_1 structure function. *Phys. Rev. C*, 89:045203, 2014. doi: 10.1103/PhysRevC.89.045203.

[65] N. Fomin et al. Scaling of the F_2 structure function in nuclei and quark distributions at $x > 1$. *Phys. Rev. Lett.*, 105:212502, 2010. doi: 10.1103/PhysRevLett.105.212502.

[66] J. Arrington, D.W. Higinbotham, G. Rosner, and M. Sargsian. Hard probes of short-range nucleon–nucleon correlations. *Prog. Part. Nucl. Phys.*, 67(4):898–938, 2012. doi: https://doi.org/10.1016/j.ppnp.2012.04.002.

[67] L.L. Frankfurt, M.M. Sargsian, and M.I Strikman. Recent observation of short range nucleon correlations in nuclei and their implications for the structure of nuclei and neutron stars. *Int. J. Mod. Phys. A*, 23(20):2991–3055, 2008. doi: 10.1142/s0217751x08041207.

[68] A.J. Freese, W. Cosyn, and M.M. Sargsian. QCD evolution of superfast quarks. *Phys. Rev. D*, 99:114019, 2019. doi: 10.1103/PhysRevD.99.114019.

[69] A.J. Freese, M.M. Sargsian, and M.I. Strikman. Probing superfast quarks in nuclei through dijet production at the LHC. *Eur. Phys. J. C*, 75(11), nov 2015. doi: 10.1140/epjc/s10052-015-3755-4.

[70] W. Boeglin and M.M. Sargsian. Modern Studies of the Deuteron: from the Lab Frame to the Light Front. *Int. J. Mod. Phys. E*, 24(03):1530003, 2015. doi: 10.1142/S0218301315300039.

[71] C. Yero et al. Probing the deuteron at very large internal momenta. *Phys. Rev. Lett.*, 125:262501, 2020. doi: 10.1103/PhysRevLett.125.262501.

[72] M.M. Sargsian, D.B. Day, L.L. Frankfurt, and M.I. Strikman. Searching for three-nucleon short-range correlations. *Phys. Rev. C*, 100(4), 2019. doi: 10.1103/physrevc.100.044320.

[73] D.B. Day, L.L. Frankfurt, M.M. Sargsian, and M.I. Strikman. Toward observation of three-nucleon short-range correlations in high-$Q^2 a(e,e^{'})x$ reactions. *Phys. Rev. C*, 107:014319, 2023. doi: 10.1103/PhysRevC.107.014319.

[74] N. Fomin, D. Higinbotham, M. Sargsian, and P. Solvignon. New results on short-range correlations in nuclei. *Ann. Rev. Nucl. Part. Sci.*, 67(1):129–159, 2017. doi: 10.1146/annurev-nucl-102115-044939.

[75] M.M. Sargsian, T.V. Abrahamyan, M.I. Strikman, and L.L. Frankfurt. Exclusive electrodisintegration of ^{3}He at high Q^2. I. generalized eikonal approximation. *Phys. Rev. C*, 71:044614, 2005. doi: 10.1103/PhysRevC.71.044614.

[76] M.M. Sargsian, T.V. Abrahamyan, M.I. Strikman, and L.L. Frankfurt. Exclusive electrodisintegration of ^{3}He at high Q^2. II. decay function formalism. *Phys. Rev. C*, 71(4), 2005. doi: 10.1103/physrevc.71.044615.

[77] R. Cruz-Torres et al. Probing few-body nuclear dynamics via ^{3}H and ^{3}He $(e, e^{'}p)$pn cross-section measurements. *Phys. Rev. Lett.*, 124(21), 2020. doi: 10.1103/physrevlett.124.212501.

[78] I. C. Cloët, W. Bentz, and A. W. Thomas. Parity-violating deep inelastic scattering and the flavor dependence of the EMC effect. *Phys. Rev. Lett.*, 109:182301, 2012. doi: 10.1103/PhysRevLett.109.182301.

[79] S. Tkachenko et al. Measurement of the structure function of the nearly free neutron using spectator tagging in inelastic ^{2}H(e, e'p)X scattering with CLAS. *Phys. Rev. C*, 89:045206, 2014. doi: 10.1103/PhysRevC.89.045206. [Addendum: Phys.Rev.C 90, 059901 (2014)].

[80] S.A. Kulagin and R. Petti. Global study of nuclear structure functions. *Nucl. Phys. A*, 765(1):126–187, 2006. doi: https://doi.org/10.1016/j.nuclphysa.2005.10.011.

[81] S.A. Kulagin and R. Petti. Structure functions for light nuclei. *Phys. Rev. C*, 82:054614, 2010. doi: 10.1103/PhysRevC.82.054614.

[82] I.C. Cloët et al. Exposing novel quark and gluon effects in nuclei. *J. Phys. G: Nucl. Part. Phys.*, 46 (9):093001, jul 2019. doi: 10.1088/1361-6471/ab2731.

[83] W.K. Brooks et al. The EMC effect in spin structure functions. E12-14-001 Experiment, 2014.

[84] S. Tronchin, H.H. Matevosyan, and A.W. Thomas. Polarized EMC effect in the QMC model. *Phys. Lett. B*, 783:247–252, 2018. doi: https://doi.org/10.1016/j.physletb.2018.06.065.

[85] H. Fanchiotti, C. A. García-Canal, T. Tarutina, and V. Vento. Medium Effects in DIS from Polarized Nuclear Targets. *Eur. Phys. J. A*, 50:116, 2014. doi: 10.1140/epja/i2014-14116-8.

[86] J.R. Smith and G.A. Miller. Polarized quark distributions in nuclear matter. *Phys. Rev. C*, 72:022203, 2005. doi: 10.1103/PhysRevC.72.022203.

[87] I.C. Cloët, W. Bentz, and A.W. Thomas. Spin-dependent structure functions in nuclear matter and the polarized emc effect. *Phys. Rev. Lett.*, 95:052302, 2005. doi: 10.1103/PhysRevLett.95.052302.

[88] I.C. Cloët, W. Bentz, and A.W. Thomas. EMC and polarized EMC effects in nuclei. *Physics Letters B*, 642(3):210–217, 2006. ISSN 0370-2693. doi: https://doi.org/10.1016/j.physletb.2006.08.076.

[89] W. Armstrong et al. Partonic structure of light nuclei. arXiv:1708.00888, 2017.

[90] W. Armstrong et al. Tagged EMC measurements on light nuclei. arXiv:1708.00891, 2017.

[91] W. Armstrong et al. Spectator-tagged deeply virtual compton scattering on light nuclei. arXiv:1708.00835, 2017.

[92] R. Dupré and S. Scopetta. 3d structure and nuclear targets. *Eur. Phys. J. A*, 52(6), 2016. doi: 10.1140/epja/i2016-16159-1.

[93] M. Hattawy et al. First Exclusive Measurement of Deeply Virtual Compton Scattering off ^{4}He: Toward the 3D Tomography of Nuclei. *Phys. Rev. Lett.*, 119(20):202004, 2017. doi: 10.1103/PhysRevLett.119.202004.

[94] M. Hattawy et al. Exploring the Structure of the Bound Proton with Deeply Virtual Compton Scattering. *Phys. Rev. Lett.*, 123(3):032502, 2019. doi: 10.1103/PhysRevLett.123.032502.

[95] R. Dupré et al. Measurement of deeply virtual Compton scattering off ^{4}He with the CEBAF Large Acceptance Spectrometer at Jefferson Lab. *Phys. Rev. C*, 104(2):025203, 2021. doi: 10.1103/PhysRevC.104.025203.

[96] O. Hen, G.A. Miller, E. Piasetzky, and L.B. Weinstein. Nucleon-Nucleon Correlations, Short-lived Excitations, and the Quarks Within. *Rev. Mod. Phys.*, 89(4):045002, 2017. doi: 10.1103/RevModPhys.89.045002.

[97] L.B. Weinstein, E. Piasetzky, D.W. Higinbotham, J. Gomez, O. Hen, and R. Shneor. Short Range Correlations and the EMC Effect. *Phys. Rev. Lett.*, 106:052301, 2011. doi: 10.1103/PhysRevLett.106.052301.

[98] A. S. Carroll et al. Nuclear Transparency to Large Angle pp Elastic Scattering. *Phys. Rev. Lett.*, 61:1698–1701, 1988. doi: 10.1103/PhysRevLett.61.1698.

[99] A. Leksanov et al. Energy dependence of nuclear transparency in C$(p, 2p)$ scattering. *Phys. Rev. Lett.*, 87:212301, 2001. doi: 10.1103/PhysRevLett.87.212301.

[100] D. Abbott et al. Quasifree $(e, e'p)$ reactions and proton propagation in nuclei. *Phys. Rev. Lett.*, 80:5072–5076, 1998. doi: 10.1103/PhysRevLett.80.5072.

[101] K. Garrow et al. Nuclear transparency from quasielastic $A(e, e^{'}p)$ reactions up to $Q^2 = 8.1(\mathrm{GeV}/c)^2$. *Phys. Rev. C*, 66:044613, 2002. doi: 10.1103/PhysRevC.66.044613.

[102] D. Bhetuwal, J. Matter, H. Szumila-Vance, M. L. Kabir, D. Dutta, R. Ent, et al. Ruling out color transparency in quasielastic $^{12}\mathrm{C(e, e^{'}p)}$ up to Q^2 of 14.2 $\mathrm{(GeV/c)^2}$. *Phys. Rev. Lett.*, 126:082301, 2021. doi: 10.1103/PhysRevLett.126.082301.

[103] E.M. Aitala et al. Observation of color-transparency in diffractive dissociation of pions. *Phys. Rev. Lett.*, 86:4773–4777, 2001. doi: 10.1103/PhysRevLett.86.4773.

[104] A. Airapetian et al. Q^2 dependence of nuclear transparency for exclusive ρ^0 production. *Phys. Rev. Lett.*, 90:052501, 2003. doi: 10.1103/PhysRevLett.90.052501.

[105] B. Clasie et al. Measurement of Nuclear Transparency for the $A(e, e'\pi^+)$ Reaction. *Phys. Rev. Lett.*, 99:242502, 2007. doi: 10.1103/PhysRevLett.99.242502.

[106] L. El Fassi et al. Evidence for the onset of color transparency in ρ^0 electroproduction off nuclei. *Phys. Lett. B*, 712:326–330, 2012. doi: 10.1016/j.physletb.2012.05.019.

[107] L. El Fassi. Chasing QCD Signatures in Nuclei Using Color Coherence Phenomena. *Physics*, 4(3):970–980, August 2022. doi: 10.3390/physics4030064.

[108] D. Dutta and R. Ent. Hadron propagation and color transparency at 12 GeV. Update on E12-06-107 Experiment, 2019.

[109] L. El Fassi et al. Study of color transparency in exclusive vector meson electroproduction off nuclei. Update on E12-06-106 Experiment, 2020.

[110] A. Airapetian et al. Hadron formation in deep inelastic positron scattering in a nuclear environment. *Eur. Phys. J. C*, 20:479–486, 2001. doi: 10.1007/s100520100697.

[111] A. Airapetian et al. Quark fragmentation to $\pi^{\pm}$, π^0, $K^{\pm}$, p and $\bar{p}$ in the nuclear environment. *Phys. Lett. B*, 577:37–46, 2003. doi: 10.1016/j.physletb.2003.10.026.

[112] A. Airapetian et al. Hadronization in semi-inclusive deep-inelastic scattering on nuclei. *Nucl. Phys. B*, 780:1–27, 2007. doi: 10.1016/j.nuclphysb.2007.06.004.

[113] A. Airapetian et al. Transverse momentum broadening of hadrons produced in semi-inclusive deep-inelastic scattering on nuclei. *Phys. Lett. B*, 684:114–118, 02 2010. doi: 10.1016/j.physletb.2010.01.020.

[114] A. Airapetian et al. Multidimensional Study of Hadronization in Nuclei. *Eur. Phys. J. A*, 47:113, 2011. doi: 10.1140/epja/i2011-11113-5.

[115] R. Baier, Yuri L. Dokshitzer, Alfred H. Mueller, S. Peigne, and D. Schiff. Radiative energy loss and p(T) broadening of high-energy partons in nuclei. *Nucl. Phys. B*, 484:265–282, 1997. doi: 10.1016/S0550-3213(96)00581-0.

[116] Stanley J. Brodsky and Paul Hoyer. A Bound on the energy loss of partons in nuclei. *Phys. Lett. B*, 298:165–170, 1993. doi: 10.1016/0370-2693(93)91724-2.

[117] S. Morán, R. Dupre, H. Hakobyan, M. Arratia, W. K. Brooks, A. Bórquez, A. El Alaoui, L. El Fassi, K. Hafidi, R. Mendez, T. Mineeva, S. J. Paul, et al. Measurement of charged-pion production in deep-inelastic scattering off nuclei with the CLAS detector. *Phys. Rev. C*, 105:015201, 2022. doi: 10.1103/PhysRevC.105.015201.

[118] S. J. Paul, S. Morán, M. Arratia, A. El Alaoui, H. Hakobyan, W. Brooks, et al. Observation of azimuth-dependent suppression of hadron pairs in electron scattering off nuclei. *Phys. Rev. Lett.*, 129: 182501, 2022. doi: 10.1103/PhysRevLett.129.182501.

[119] M.Yu Barabanov, M. Bedolla, W. Brooks, G.D. Cates, Ch. Chen, Y. Chen, E. Cisbani, M. Ding, G. Eichmann, R. Ent, J. Ferretti, R.W. Gothe, T. Horn, S. Liuti, C. Mezrag, A. Pilloni, A.J.R. Puckett, C.D. Roberts, P. Rossi, and B.B. Wojtsekhowski. Diquark correlations in hadron physics: Origin, impact and evidence. *Prog. Part. Nucl. Phys.*, 116:103835, 2021. doi: 10.1016/j.ppnp.2020.103835.

[120] T. Chetry, L. El Fassi, et al. First measurement of λ electroproduction off nuclei in the current and target fragmentation regions. arXiv:2210.13691, 2022.

[121] W. K. Brooks et al. Quark propagation and hadron formation. E12-06-117 Experiment, 2010.

[122] C. Cocuzza, W. Melnitchouk, A. Metz, and N. Sato. Polarized antimatter in the proton from a global QCD analysis. *Phys. Rev. D*, 106(3):L031502, 2022. doi: 10.1103/PhysRevD.106.L031502.

[123] Tianbo Liu, W. Melnitchouk, Jian-Wei Qiu, and N. Sato. Factorized approach to radiative corrections for inelastic lepton-hadron collisions. *Phys. Rev. D*, 104(9):094033, 2021. doi: 10.1103/PhysRevD.104.094033.

[124] J. R. McKenney, Nobuo Sato, W. Melnitchouk, and Chueng-Ryong Ji. Pion structure function from leading neutron electroproduction and SU(2) flavor asymmetry. *Phys. Rev. D*, 93(5):054011, 2016. doi: 10.1103/PhysRevD.93.054011.

[125] P. C. Barry, N. Sato, W. Melnitchouk, and Chueng-Ryong Ji. First Monte Carlo Global QCD Analysis of Pion Parton Distributions. *Phys. Rev. Lett.*, 121(15):152001, 2018. doi: 10.1103/PhysRevLett.121.152001.

[126] P. C. Barry, Chueng-Ryong Ji, N. Sato, and W. Melnitchouk. Global QCD Analysis of Pion Parton Distributions with Threshold Resummation. *Phys. Rev. Lett.*, 127(23):232001, 2021. doi: 10.1103/PhysRevLett.127.232001.

[127] P. A. Zyla et al. Review of Particle Physics. *PTEP*, 2020(8):083C01, 2020. doi: 10.1093/ptep/ptaa104.

[128] R. L. Workman et al. Review of Particle Physics. *PTEP*, 2022:083C01, 2022. doi: 10.1093/ptep/ptac097.

[129] Liping Gan, Bastian Kubis, Emilie Passemar, and Sean Tulin. Precision tests of fundamental physics with η and η' mesons. *Phys. Rept.*, 945:1–105, 2022. doi: 10.1016/j.physrep.2021.11.001.

[130] Martin Hoferichter, Bai-Long Hoid, Bastian Kubis, Stefan Leupold, and Sebastian P. Schneider. Pion-pole contribution to hadronic light-by-light scattering in the anomalous magnetic moment of the muon. *Phys. Rev. Lett.*, 121(11):112002, 2018. doi: 10.1103/PhysRevLett.121.112002.

[131] A. Browman, J. DeWire, B. Gittelman, K. M. Hanson, E. Loh, and R. Lewis. The Radiative Width of the eta Meson. *Phys. Rev. Lett.*, 32:1067, 1974. doi: 10.1103/PhysRevLett.32.1067.

[132] M. Tanabashi et al. Review of Particle Physics. *Phys. Rev. D*, 98(3):030001, 2018. doi: 10.1103/PhysRevD.98.030001.

[133] A. Kastner and H. Neufeld. The K(l3) scalar form factors in the standard model. *Eur. Phys. J. C*, 57: 541–556, 2008. doi: 10.1140/epjc/s10052-008-0703-6.

[134] D. Giusti, V. Lubicz, C. Tarantino, G. Martinelli, F. Sanfilippo, S. Simula, and N. Tantalo. Leading isospin-breaking corrections to pion, kaon and charmed-meson masses with Twisted-Mass fermions. *Phys. Rev. D*, 95(11):114504, 2017. doi: 10.1103/PhysRevD.95.114504.

[135] I. Larin et al. Precision measurement of the neutral pion lifetime. *Science*, 368(6490):506–509, 2020. doi: 10.1126/science.aay6641.

[136] A. M. Bernstein and Barry R. Holstein. Neutral Pion Lifetime Measurements and the QCD Chiral Anomaly. *Rev. Mod. Phys.*, 85:49, 2013. doi: 10.1103/RevModPhys.85.49.

[137] J. L. Goity, A. M. Bernstein, and B. R. Holstein. The Decay pi0 —> gamma gamma to next to leading order in chiral perturbation theory. *Phys. Rev. D*, 66:076014, 2002. doi: 10.1103/PhysRevD.66.076014.

[138] B. Ananthanarayan and B. Moussallam. Electromagnetic corrections in the anomaly sector. *JHEP*, 05:052, 2002. doi: 10.1088/1126-6708/2002/05/052.

[139] Karol Kampf and Bachir Moussallam. Chiral expansions of the pi0 lifetime. *Phys. Rev. D*, 79:076005, 2009. doi: 10.1103/PhysRevD.79.076005.

[140] B. L. Ioffe and A. G. Oganesian. Axial anomaly and the precise value of the pi0 —> 2 gamma decay width. *Phys. Lett. B*, 647:389–393, 2007. doi: 10.1016/j.physletb.2007.02.021.